

## Research Article

# Modelling and Analysis of a Host-Parasitoid Impulsive Ecosystem under Resource Limitation

Peipei Wang,<sup>1</sup> Wenjie Qin ,<sup>1,2</sup> and Guangyao Tang<sup>3</sup>

<sup>1</sup>Three Gorges Mathematical Research Center, China Three Gorges University, Yichang 443002, China

<sup>2</sup>Laboratory for Industrial and Applied Mathematics, York University, Toronto M3J 1P3, Canada

<sup>3</sup>Department of Mathematics, Hubei Minzu University, Enshi 445000, China

Correspondence should be addressed to Wenjie Qin; [wenjiejieqin@hotmail.com](mailto:wenjiejieqin@hotmail.com)

Received 16 November 2018; Accepted 26 December 2018; Published 14 January 2019

Academic Editor: Toshikazu Kuniya

Copyright © 2019 Peipei Wang et al. This is an open access article distributed under the Creative Commons Attribution License, which permits unrestricted use, distribution, and reproduction in any medium, provided the original work is properly cited.

With a long history of theoretical development, biological model has focused on the interaction of a parasitoid and its host. In this paper, two Nicholson-Bailey models with a nonlinear pulse control strategy are proposed and analyzed to examine how limited resource affects the pest control. For a fixed-time discrete impulsive model, the existence and stability of the host-free periodic solution are derived. Threshold analysis suggests that it is critical to release parasitoid in an optimal number in case of the happening of the intra-specific competition, which will seriously affect the pest control. Bifurcation analysis reveals that the model exists complex dynamics including period doubling, chaotic solutions, coexistence of multiple attractors, and so on. For a state-dependent discrete impulsive model, the numerical simulations for bifurcation analysis are studied, the results show that how the key parameters and the initial densities of both populations affect the pest outbreaks, and consequently the relative biological implications with respect to pest control are discussed.

## 1. Introduction

Mathematical models can assist in the design and understanding of basic problems in biology, medicine, and life sciences, which can take many forms including dynamical system, differential equation, difference equation, and so on [1–3]. Different models can describe different biological phenomena, with each having different strengths. Some certain species, including many species of insect, have no overlap between successive generations and so their populations evolve in discrete time-steps. The discrete model governed by a difference equation is more appropriate than the continuous ones taking into account the fact that the population has a short life expectancy, non-overlapping generations in the real world [4–6], so it is reasonable to study biological models governed by difference equations [7–13].

The insect pests' outbreaks often cause serious ecological and economic problems, requiring complex control measures to reduce the harm brought by insect pests of agriculture and insect vectors of important plant, animal, and human diseases. In order to control pest more effective, at the same

time, environmental influences and human interventions are taken into consideration, and the concept of Integrated Pest Management (IPM) strategy has been proposed [14–17], as a consequence it is challenging to evaluate the effectiveness of control measures such as biological (releasing predators), chemical (spraying pesticides), and physical control tactics. Based on the concept of IPM strategy, some mathematical models to describe the interaction between the pest and its natural enemy have been developed [18–21].

One of the IPM strategies is to release natural enemies and spray chemical pesticides at a fixed time, since pesticides can quickly kill a significant portion of a pest population, and it is convenient to carry out. Meanwhile, the IPM strategy can be applied more effectively to achieve maximum effect at the minimum levels of pesticide if the life cycle of a pest is understood; i.e., it is used when the pest is at its most vulnerable. Pesticides can be relatively cheap and easy to apply and fast-acting and in most instances can be relied on to control the pests. Therefore, the periodic control strategy has been applied widely and extended in agriculture and ecology [18, 19].

Another important concept in IPM strategy is the Threshold Policy Control (TPC) [22, 23], which maintains the pests' density below the Economic Injury Level (EIL) [24–26] by releasing predators and spraying pesticides once the pests' density reaches the Economic Threshold (ET) [27, 28]; it is also called by state-dependent feedback control. As we know, the main purpose of IPM is to maintain the density of the pests below the EIL rather than seeking to eradicate them, and the suitable tactic can be applied only when the density of pests reaches the given ET; it can minimize the damage of insecticides to non-target pests and preserve the quality of the environment. Therefore the state-dependent impulsive dynamical model could be appropriate to describe such control tactics [20, 21].

However, the above IPM strategy has assumed that the killing rate of pesticide is a constant, which shows that the agricultural resources including chemical pesticides, labor forces, facilities, and costs are very effective and sufficient for pest control. In reality, every community or country has an appropriate or limited capacity for pesticides, costs, etc., especially for developing countries. Although it is critical to understand resource limitation to effective management and conservation of populations, limited resource is difficult to quantify partly because it is a dynamic process [29–32]. The main purpose of this paper is to describe the limited resources based on the classic Nicholson-Bailey model [33]; there are two different models with IPM strategies being derived. In order to characterize the saturation phenomenon of the limited resources, the constant fatality rate is replaced with a nonlinear saturation function which depends on its population density. Some theoretical, numerical, biological analyses are given to investigate how limited resources affect host outbreaks.

The organization of the present paper is as follows: in the next section, a fixed-time impulsive control for a Nicholson-Bailey model with resource limitation is proposed; by employing the qualitative analysis and the discrete dynamical system determined by the stroboscopic map, the threshold conditions which guarantee the existence and stability of the host-free periodic solution are obtained. Meanwhile, 1-dimensional bifurcation analyses are investigated; the key parameters and initial values of both populations affect the pest outbreaks are given by taking advantage of numerical simulation. In Section 3, we describe a Nicholson-Bailey ecosystem with resource limitation by state-dependent impulsive control; by employing numerical simulations, the model is analyzed to understand how resource limitation affects pest population outbreaks; the intersection between the initial densities and pest control will be discussed. The paper ends with some interesting biological conclusions, which complement the theoretical findings.

## 2. Fixed-Time Impulsive Control for a Nicholson-Bailey Model with Resource Limitation

*2.1. Model Formulation.* In 1935, Nicholson and Bailey [33] proposed a classic discrete host-parasitoid model, as an

intergenerational survival rate for parasitoids was considered. In 2008, Tang [8] extended the basic Nicholson-Bailey model as follows:

$$\begin{aligned} H_{n+1} &= H_n \exp[r - aP_n], \\ P_{n+1} &= H_n [1 - \exp(-aP_n)] + \sigma P_n. \end{aligned} \quad (1)$$

Here  $H_n$  and  $P_n$  represent the density of hosts(or pests) and parasitoids(or natural enemies) at  $n$ -th generation, respectively;  $r$  is the intrinsic growth rate for the host population;  $a$  denotes the searching efficiency of the parasitoid population; the terms  $\exp(-aP_n)$  and  $[1 - \exp(-aP_n)]$  represent the probability that the host succeeds and fails in escaping from the parasitism, respectively;  $\sigma$  is the density-independent survival of the parasitoid at  $n$ -th generation,  $n \in \mathcal{I} \triangleq \{0, 1, 2, \dots\}$ .

In order to investigate the dynamics of system (1) with IPM strategies, by introducing periodic spraying pesticide only for hosts, and releasing parasitoids, Tang [8] proposed the following Nicholson-Bailey model:

$$\begin{aligned} H_{n+1} &= H_n \exp[r - aP_n], \\ P_{n+1} &= H_n [1 - \exp(-aP_n)] + \sigma P_n, \\ & n \in \mathcal{I} \\ H_{qk^+} &= (1 - q_1) H_{qk}, \\ P_{qk^+} &= (1 + q_2) P_{qk} + \tau, \\ & q, k \in \mathcal{N} \end{aligned} \quad (2)$$

with the initial densities  $(H_{0^+}, P_{0^+}) = (H_0, P_0)$  and  $\mathcal{N} \triangleq \{1, 2, \dots\}$ . Meanwhile,  $q \in \mathcal{N}$  is the pulse period,  $q_1$  is the killing rate for hosts, and  $q_2$  and  $\tau$  are the release rate and constant for parasitoids at  $qk$ -th generation, respectively.  $H_{qk}$  and  $P_{qk}$  ( $H_{qk^+}$  and  $P_{qk^+}$ ) denote the densities of both populations at  $qk$ -th generation before (after) the impulsive perturbations, respectively.

Now, taking into account the resource limitation and saturation effects, that is, a linear pulse in model (2) is replaced with a saturation phenomenon of limited resources; especially, a Hill function [34] is used to describe the resource limitation. For convenience and simplification, model (2) can be rewritten as

$$\begin{aligned} H_{n+1} &= H_n \exp[r - aP_n], \\ P_{n+1} &= H_n [1 - \exp(-aP_n)] + \sigma P_n, \\ & n \in \mathcal{I}, \end{aligned}$$

$$\begin{aligned}
H_{qk^+} &= \left(1 - \frac{q_1^{\max} H_{qk}}{\theta_1 + H_{qk}}\right) H_{qk}, \\
P_{qk^+} &= \left(1 + \frac{q_2^{\max} P_{qk}}{\theta_2 + P_{qk}}\right) P_{qk} + \tau, \\
q, k &\in \mathcal{N},
\end{aligned} \tag{3}$$

where  $q_1^{\max}$  and  $\theta_1$  represent the maximal fatality rate and the half-saturation constant for hosts, respectively.  $q_2^{\max}$  and  $\theta_2$  represent the maximal release rate and the half-saturation constant for parasitoids, respectively. Assume that  $0 \leq q_i^{\max} < 1$  and  $\theta_i > 0$  for  $i = 1, 2$ .

**2.2. Mathematical Analysis of the Host-Free Periodic Solution and Threshold Conditions.** With the main purpose of IPM strategy, it is necessary to illustrate the existence of the host-free periodic solution of model (3) and focus on determining its global attractivity. In order to do this, we first investigate the host-free set:  $\mathcal{A} = \{(H, P) \in \mathcal{R}_+^2, H = 0\}$ , which is clearly invariant by model (3); it follows from model (3) and its pest-free set  $\mathcal{A}$  that

$$\begin{aligned}
P_{n+1} &= \sigma P_n, \quad n \in \mathcal{L}, \\
P_{qk^+} &= \left(1 + \frac{q_2^{\max} P_{qk}}{\theta_2 + P_{qk}}\right) P_{qk} + \tau, \quad k \in \mathcal{N}, \\
P_0^+ &= P_0.
\end{aligned} \tag{4}$$

Obviously, model (4) is a periodic system, so the periodic solution  $P_n$  can be defined at the subinterval  $[qs^+, q(s+1))$  with the initial value  $P_{qs^+}$ ,  $s \in \mathcal{L}$ . Noting that  $P_{qs^+}$  represents the parasitoid's density after the impulsive perturbation.

From the first equation of model (4), we can use this iteration equation at interval  $[qs^+, q(s+1))$  and obtain  $P_{n+1} = \sigma^{n+1-qs} P_{qs^+}$ . Especially, it gives that  $P_{q(s+1)} = \sigma^q P_{qs^+}$  as  $n = q(s+1) - 1$ .

Now, combining the second equation of model (4) and the above one yields

$$P_{q(s+1)^+} = \frac{(q_2^{\max} + 1) \sigma^{2q} P_{qs^+}^2 + (\theta_2 + \tau) \sigma^q P_{qs^+} + \theta_2 \tau}{\theta_2 + \sigma^q P_{qs^+}}. \tag{5}$$

Denoting  $P_{q(s+1)^+}$  as  $P_{n+1}$ , then the above equation can be rewritten as the following difference equation:

$$\begin{aligned}
P_{n+1} &= \mathcal{F}(P_n) \\
&\triangleq \frac{(1 + q_2^{\max}) \sigma^{2q} P_n^2 + (\theta_2 + \tau) \sigma^q P_n + \theta_2 \tau}{\theta_2 + \sigma^q P_n}.
\end{aligned} \tag{6}$$

Equation (6) is a stroboscopic map of model (4): it describes the relations of the parasitoids' density between any two successive pulse points; that is, the existence of a positive steady state of (6) represents the existence of a positive periodic solution of model (4). Therefore, we first explore the

positive steady state of the stroboscopic map (6); let us get the derivative of  $\mathcal{F}(P_n)$  with  $P_n$  and yield

$$\begin{aligned}
\mathcal{F}'(P_n) &= \frac{(q_2^{\max} + 1) \sigma^{3q} P_n^2 + 2(q_2^{\max} + 1) \sigma^{2q} \theta_2 P_n + \theta_2^2 \sigma^q}{\sigma^{2q} P_n^2 + 2\theta_2 \sigma^q P_n + \theta_2^2}.
\end{aligned} \tag{7}$$

According to the stability theory of differential equation, it is necessary to ensure that the inequality  $|\mathcal{F}'(P_n)| < 1$  holds true, and this condition is equivalent to

$$A_0 P_n^2 + B_0 P_n + C_0 < 0, \tag{8}$$

where  $A_0 = \sigma^{2q} [(1 + q_2^{\max}) \sigma^q - 1]$ ,  $B_0 = 2\theta_2 \sigma^q [(1 + q_2^{\max}) \sigma^q - 1]$ ,  $C_0 = \theta_2^2 (\sigma^q - 1)$ . By a simple calculation, one yields  $\Delta_0 = B_0^2 - 4A_0 C_0 = 4\theta_2^2 q_2^{\max} \sigma^q A_0$ . It is easy to find that if  $A_0 < 0$  holds true, then  $\Delta_0 < 0$ , which implies  $|\mathcal{F}'(P_n)| < 1$ . For simplification,  $A_0 < 0$  can be rewritten as

$$\mathcal{R}_1 \triangleq (1 + q_2^{\max}) \sigma^q < 1. \tag{9}$$

The above inequality can ensure the stability of a positive solution of the stroboscopic map (6). Meanwhile, it also plays an important role in discussing the existence of the positive fixed point for (6).

Next, we continue to investigate the positive fixed point of the stroboscopic map (6). For convenience, we denote this fixed point by  $\tilde{P}$ ; then it follows from the stroboscopic map (6) that

$$\tilde{P} = \frac{(1 + q_2^{\max}) \sigma^{2q} \tilde{P}^2 + (\theta_2 + \tau) \sigma^q \tilde{P} + \theta_2 \tau}{\theta_2 + \sigma^q \tilde{P}}, \tag{10}$$

which means

$$A_1 \tilde{P}^2 + B_1 \tilde{P} + C_1 = 0, \tag{11}$$

where  $A_1 = \sigma^q [(1 + q_2^{\max}) \sigma^q - 1]$ ,  $B_1 = (\theta_2 + \tau) \sigma^q - \theta_2$ ,  $C_1 = \theta_2 \tau > 0$ . Obviously, we can obtain that  $A_1 < 0$  and  $\Delta_1 = B_1^2 - 4A_1 C_1 > 0$  as  $\mathcal{R}_1 < 1$  holds true. That is, the stroboscopic map (6) exists in only one positive fixed point  $\tilde{P} = -(B_1 + \sqrt{\Delta_1}) / (2A_1)$ . Therefore, we have the following result.

**Lemma 1.** *Model (4) exists as a positive periodic solution  $P_n^*$  provided that  $\mathcal{R}_1 < 1$  holds true. Meanwhile, for every positive solution  $P_n$  of model (4), it is given that  $\lim_{n \rightarrow +\infty} |P_n - P_n^*| = 0$ . Here  $P_n^* = \sigma^{n-qs} \tilde{P}$  with  $n \in [qs^+, q(s+1))$ ,  $s \in \mathcal{L}$ .*

Based on Lemma 1, we can obtain the general expression of the host-free periodic solution of model (3) in the interval  $[qs^+, q(s+1))$  for all  $s \in \mathcal{L}$  denoted by

$$(0, P_n^*) = \left(0, -\sigma^{n-qs} \frac{B_1 + \sqrt{\Delta_1}}{2A_1}\right). \tag{12}$$

In order to investigate the global stability of the host-free periodic solution  $(0, P_n^*)$  of model (3), the following theorem is derived.

**Theorem 2.** Let  $(H_n, P_n)$  be any positive solution of model (3); the host-free periodic solution  $(0, P_n^*)$  of model (3) is globally asymptotically stable in the first quadrant, provided that

$$\mathcal{R}_2 \triangleq \frac{2qrA_1(1-\sigma)}{a(1-\sigma^q)(B_1 + \sqrt{\Delta_1})} < 1. \quad (13)$$

*Proof.* To prove Theorem 2, the following condition (16) is considered first. It follows from  $\mathcal{R}_2 < 1$ , model (3), and  $P_n^* = \sigma^{n-qs} \tilde{P}$  that we have

$$\sum_{n=qs}^{q(s+1)-1} (r - aP_n^*) < 0, \quad (14)$$

which implies

$$\prod_{n=qs}^{q(s+1)-1} \exp(r - aP_n^*) < 1. \quad (15)$$

Therefore, from the above inequality, we can assume that there exists a sufficiently small positive  $\varepsilon$  such that

$$\sigma_1 \triangleq \prod_{n=qs}^{q(s+1)-1} \exp[r - a(P_n^* - \varepsilon)] < 1. \quad (16)$$

Next, we continue to prove Theorem 2. Obviously, it is easy to show that  $P_{n+1} > \sigma P_n$ . Then the following comparison equation with pulse is considered.

$$\begin{aligned} Q_{n+1} &= \sigma Q_n, \quad n \in \mathcal{X}, \\ Q_{qk^+} &= \left(1 + \frac{q_2^{\max} Q_{qk}}{\theta_2 + Q_{qk}}\right) Q_{qk} + \tau, \quad k \in \mathcal{N}. \end{aligned} \quad (17)$$

By using Lemma 1, it gives that  $P_n \geq Q_n$  and  $\lim_{n \rightarrow +\infty} Q_n = P_n^*$ . Hence, for all  $n \in \mathcal{X}$ , the inequality  $P_n \geq Q_n > P_n^* - \varepsilon$  holds true. Then according to model (3), we have

$$\begin{aligned} H_{n+1} &\leq H_n \exp[r - a(P_n^* - \varepsilon)], \quad n \in \mathcal{X}, \\ H_{qk^+} &= \left(1 - \frac{q_1^{\max} H_{qk}}{\theta_1 + H_{qk}}\right) H_{qk}, \quad k \in \mathcal{N}. \end{aligned} \quad (18)$$

Associated with the condition (16), the following inequality is derived:

$$\begin{aligned} H_{q(s+1)} &\leq H_{qs^+} \prod_{n=qs}^{q(s+1)-1} \exp[r - a(P_n^* - \varepsilon)] \\ &= H_{qs} \left(1 - \frac{q_1^{\max} H_{qs}}{\theta_1 + H_{qs}}\right)^{q(s+1)-1} \prod_{n=qs}^{q(s+1)-1} \exp[r - a(P_n^* - \varepsilon)] \quad (19) \\ &< H_{qs} \prod_{n=qs}^{q(s+1)-1} \exp[r - a(P_n^* - \varepsilon)] = \sigma_1 H_{qs}, \end{aligned}$$

so it is easy to show that  $H_{qs} \leq H_0 + \sigma_1^s$  and  $\lim_{s \rightarrow +\infty} H_{qs} = 0$ . It follows from model (3) that  $0 \leq H_n \leq H_{n-1} \exp r$ , and, for any  $n \in [qs^+, q(s+1))$ , we have

$$\begin{aligned} 0 \leq H_n &\leq \exp[(n-qs)r] H_{qs^+} \\ &\leq \left(1 - \frac{q_1^{\max} H_{qs}}{\theta_1 + H_{qs}}\right) \exp(qr) H_{qs}, \end{aligned} \quad (20)$$

in other words,  $\lim_{n \rightarrow +\infty} H_n = 0$ .

Thus, we have proved the global stability of the host-free periodic solution  $(0, P_n^*)$  of model (3). This completes the proof.  $\square$

Based on Theorem 2, the global stability of the host-free periodic solution of model (3) is determined by  $\mathcal{R}_1 < 1$  and  $\mathcal{R}_2 < 1$ ; that is, it is crucial that those two threshold values make great effects on the dynamics of model (3). Therefore, in the following, we employ  $\mathcal{R}_1$  and  $\mathcal{R}_2$  to investigate the important factors which affect the threshold values most significantly by numerical simulations.

As we know, resource limitation exists extensively in pest control, especially in some developing countries. There are so many factors affecting the limited resource; this study focuses on the thresholds  $\mathcal{R}_1$  and  $\mathcal{R}_2$  which ensure the existence and stability of host-free periodic solution, and those thresholds will directly influence the success of pest control. According to the expressions of  $\mathcal{R}_1$  and  $\mathcal{R}_2$ , the impulsive periodic  $q$ , the maximal release rate  $q_2^{\max}$ , and the half saturation constant  $\theta_2$  for parasitoid population are the key parameters that affect  $\mathcal{R}_1$ ,  $\mathcal{R}_2$  and the limited resource. In Figure 1(a), with the increasing of the pulse periodic  $q$ , the threshold  $\mathcal{R}_1$  decreases, while the curve of  $\mathcal{R}_2 - q$  is a typical single-peak curve. And only if the pulse periodic  $q > 4$ ,  $\max\{\mathcal{R}_1, \mathcal{R}_2\} < 1$  holds true, then the host-free periodic solution  $(0, P_n^*)$  can become stable. The higher the frequency of a control measure is, the lower the pulse periodic  $q$  is. Figure 1(a) indicates that the pest can be out of control by increasing the control frequency (i.e., decreasing the control periodic  $q$ ), and it is not even realistic to do under the limited resource.

Meanwhile, the optimal release rate of parasitoid  $q_2^{\max}$  is between 0.34 and 0.90 which ensures  $\mathcal{R}_2 < 1$ , as shown in Figure 1(b). Based on this fact, it is crucial to choose a proper  $q_2^{\max}$  to direct the adaptive resource allocation, especially under the limited control resource. To release the excessive parasitoid may not be good for pest control and will also bring about some other problems such as intra-specific competition for parasitoid population. Analogously, the curve of  $\mathcal{R}_2 - \theta_2$  shown in Figure 1(c) can also confirm this result, and Figure 1(c) shows that (1) the threshold value  $\mathcal{R}_2$  is decreased gradually with increasing of the half-saturation constant  $\theta_2$ ; (2) the critical value of  $\theta_2$  is 2.16. From Figures 1(b) and 1(c), we should take appropriate measures to prevent the releasing of parasitoid which will be beneficial to pest control, which is the optimal strategy to wrestle with enormous challenges of the limited resources.

This section mainly analyzes the host-free periodic solution; however, there are several other types of solutions for model (3), which will be useful for bifurcation analysis in the next subsection, so we list those solutions as follows.

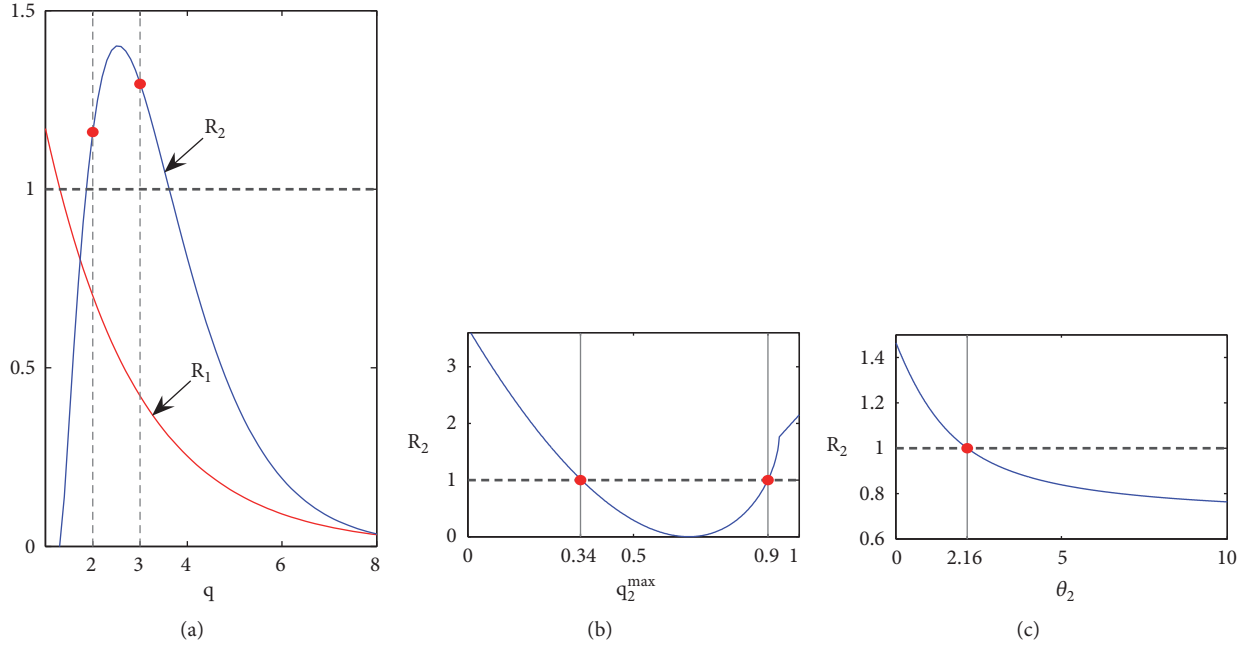


FIGURE 1: Sensitivity analysis for  $\mathcal{R}_1, \mathcal{R}_2$ . (a) The curves of  $\mathcal{R}_1$ - $q$  and  $\mathcal{R}_2$ - $q$ , parameters are  $r = 0.5, a = 0.01, q_2^{\max} = 0.95, \sigma = 0.6, \theta_2 = 0.2, \tau = 0.2$ ; (b) the curve of  $\mathcal{R}_2$ - $q_2^{\max}$  with  $r = 0.4, a = 0.05, q_2^{\max} = 0.95, \sigma = 0.6, \theta_2 = 4, \tau = 0.8, q = 1$ ; (c) the curve of  $\mathcal{R}_2$ - $\theta_2$  with  $r = 0.2, a = 0.05, q_2^{\max} = 0.3, \sigma = 0.8, \tau = 1.2, q = 2$ .

- (i) Host-free periodic solution, denoted by HF: the host population is eradicated, while the parasitoid population oscillates periodically, as shown in Figures 2(a) and 2(b), respectively, and the period of Parasitoid is 2.
- (ii) Host-parasitoid permanence periodic solution, denoted by HP: both individuals can oscillate with a periodic, as shown in Figures 2(c) and 2(d), and the period of HP is 9.
- (iii) Host-outbreak solution, denoted by HO: the host population has periodic or irregular outbreaks with large maximum amplitudes, as shown in Figures 2(e) and 2(f).

**2.3. Numerical Bifurcation Analysis.** In order to get some dynamical behaviors of model (3), a single parameter bifurcation is adopted, which can give information about the dependence of the dynamics on a certain parameter. This subsection focuses on the complex dynamics including period doubling, chaotic solutions, coexistence of multiple attractors, the basin of attraction, and so on.

Once the threshold value exceeds a critical level, that is,  $\mathcal{R}_2 \geq 1$ , the host-free solution  $(0, P_n^*)$  becomes unstable; both host and parasitoid populations can oscillate periodically with a large amplitude; a series of bifurcation phenomena will be taken place at this moment. To investigate the complex dynamics that model (3) can have, we choose the release rate  $\tau$  for parasitoids as a bifurcation parameter and fix all other parameters as those in Figure 3 for the different half-saturation constants  $\theta_1, \theta_2$ . Figures 3(a) and 3(b) are bifurcation diagrams with resource limitation, i.e.,  $\theta_1 = 9, \theta_2 = 2$ ; Figures 3(c) and 3(d) are bifurcation diagrams

without resource limitation, i.e.,  $\theta_1 = \theta_2 = 0$ . Comparing those bifurcation diagrams, we conclude that the nonlinear pulse control measure can produce more complex dynamics than the linear ones, and the limited resource plays a key role.

To illustrate the complex and interesting dynamic behaviors of model (3) more clearly, the intrinsic growth rate  $r$  and half-saturation constant  $\theta_2$  are chosen as a bifurcation parameter, respectively; numerical bifurcation analyses are derived to show some possible dynamics as shown in Figures 4 and 5. Specifically, Figure 4 shows that model (3) has periodic doubling bifurcation, periodic window, and chaos solution as the bifurcation parameters  $r \in (2, 71, 2.805), (2, 819, 2.825),$  and  $(2, 83, 2.86)$ , respectively, while model (3) has periodic adding and halving phenomenon as the bifurcation parameters  $\theta_2 \in (0, 0.65)$  and  $(0.7, 1.5)$ , respectively. Meanwhile, model (3) has some other dynamic behaviors including quasiperiodic solutions, tangent bifurcation, multistability, and chaos crisis in more sensitive parameter space. The results indicate that the parameters of model (3) are highly sensitive, and the dynamical behaviors of model (3) will have a complex change along with parameter variations, even if there is a small perturbation in some key parameters.

From the above bifurcation diagrams (Figures 3, 4, and 5), model (3) has several coexisting attractors in a special parameter space. Especially, all parameters are fixed as shown in Figure 6, model (3) has four attractors with different initial densities. Obviously, the cases in Figures 6(a) and 6(b) are a host-free and parasitoid-free solution, and the other cases shown in Figures 6(c)–6(h) are HP periodic solutions, and the maximum amplitudes of host population after the 100-th generation from top to bottom are 6.8, 10, 2, respectively. Similarly, the maximum amplitudes of parasitoid population after the 100-th generation from top to bottom

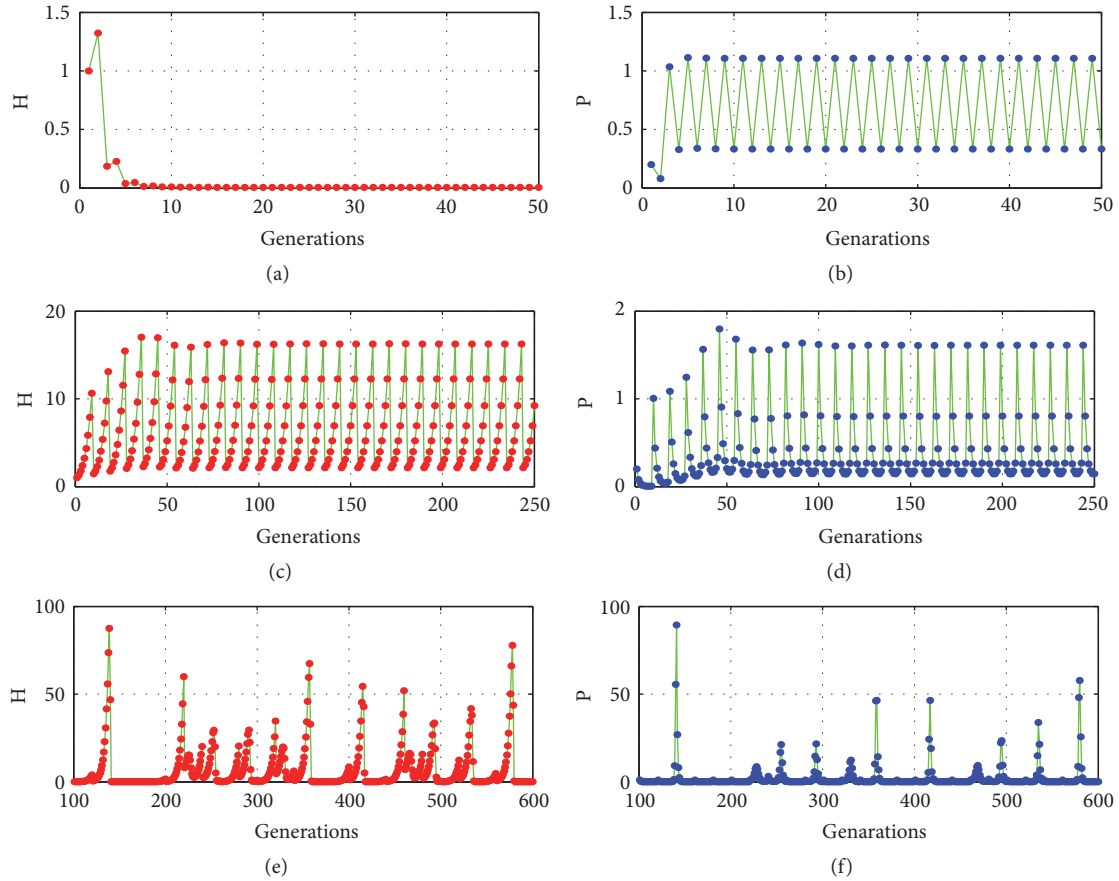


FIGURE 2: Three types of solutions for model (3). (a-b) HF periodic solution with  $q = 2$ ; (c-d) HP periodic solution with  $q = 9$ ; (e-f) HO solution with  $q = 20$ . Parameters are fixed as  $r = 0.3$ ,  $a = 0.1$ ,  $q_1^{max} = 0.9$ ,  $\theta_1 = 0.01$ ,  $q_2^{max} = 0.4$ ,  $\theta_2 = 0.5$ ,  $\tau = 1$ , and  $(H_0, P_0) = (1, 0.2)$ .

are 26.5, 30.5, 23.4, respectively. Figure 6 indicates that those phenomena are caused by different initial densities.

In order to illustrate the initial sensitivities shown in Figure 6 more specifically, the basins of attraction with respect to four different coexistence solutions are shown in Figure 7, the parameters are identical to Figure 6, and Figure 7(b) is the magnification part of Figure 7(a). The final stable states of host and parasitoid populations depend on their initial densities, the results indicate that the successful biological control depends on the initial densities of both populations. The proper initial densities can affect host outbreak and help us to design the proper control strategies as well as making management decisions.

### 3. State-Dependent Impulsive Control for a Nicholson-Bailey Model with Resource Limitation

**3.1. Model Formulation.** In Section 2, model (3) with a fixed-time impulsive control strategy has been investigated. One of the greatest advantages of this periodic control strategy is the purpose of eradicating pests rapidly and implementing easily, so it is widely applied and extended in agriculture and ecology. However, the most fatal disadvantage is that it can cause serious environmental pollution and resource waste, which defeats the purpose of IPM strategy. Especially in the

resource limitation, it is always questioned, so it is necessary to look for a new measure to control pest.

It is well known that the main purpose of IPM is to maintain the density of the pests below the EIL rather than seeking to eradicate them, and the suitable tactic will be applied only when the density of host reaches the given ET. That is the threshold control strategy. Therefore, in model (1), only when the density of pests exceeds the given threshold, the pesticide will be applied to host population and decrease its density to  $ET$ , that is

$$(1 - q_{1n})H_n \exp[r - aP_n] = ET, \quad (21)$$

where  $q_{1n}$  is the killing rate for host, and the survival rate of host after a pesticide application is  $1 - q_{1n}$ . With the idea of the threshold control strategy, we can redefine the killing rate as follows:

$$q_{1n} = \begin{cases} 1 - \frac{ET}{H_n \exp(r - aP_n)}, & \text{if } H_{n+1} > ET, \\ 0, & \text{if } H_{n+1} \leq ET. \end{cases} \quad (22)$$

By employing threshold policy control and IPM strategy, we can use the combination of the biological (releasing the parasitoid) and chemical (spraying pesticide) tactics to suppress the pest to a controllable level  $ET$ . Meanwhile, the resource limitations and saturation effects are taken into

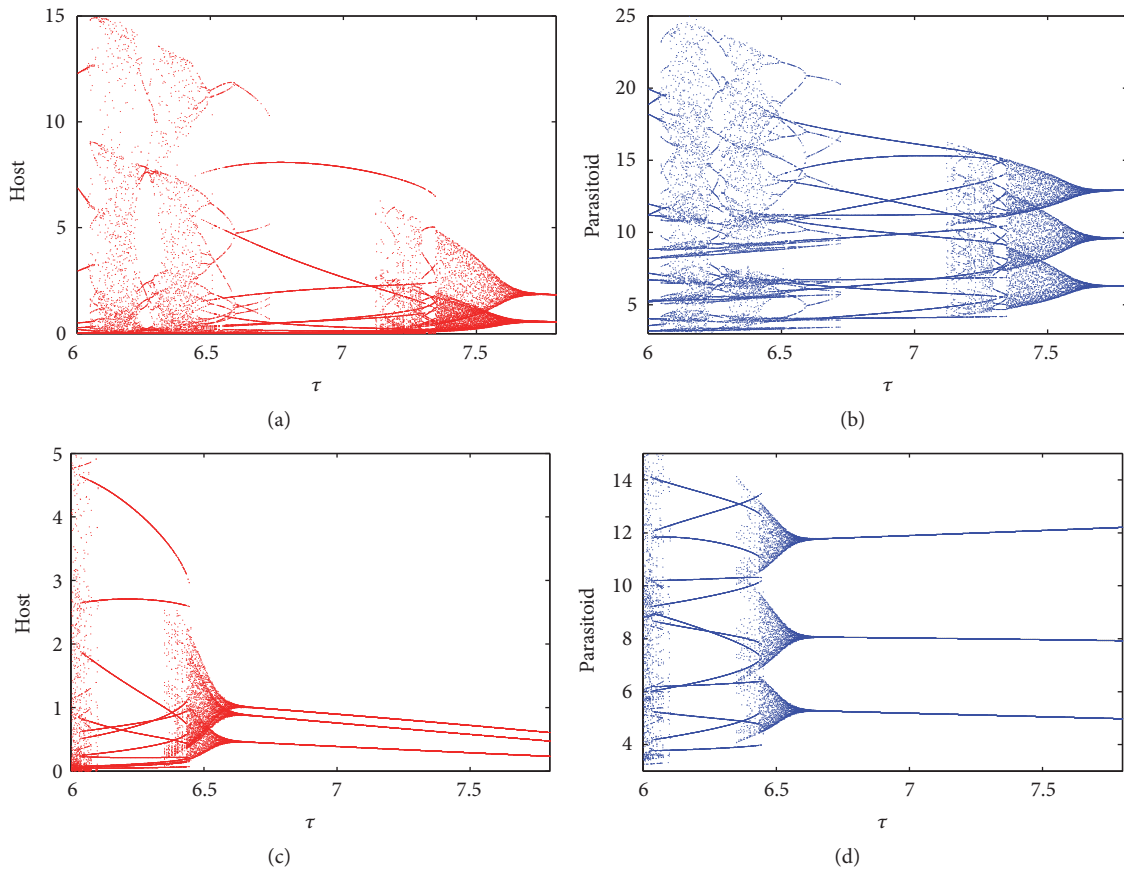


FIGURE 3: Bifurcation diagram of model (3) with  $\tau$ . Here (a) & (b) with  $\theta_1 = 9, \theta_2 = 2$ ; (c) & (d) with  $\theta_1 = \theta_2 = 0$ , and all other parameters are  $a = 0.39, r = 3.8, \sigma = 0.6, q_1^{max} = 0.8, q_2^{max} = 0.3, q = 3$ .

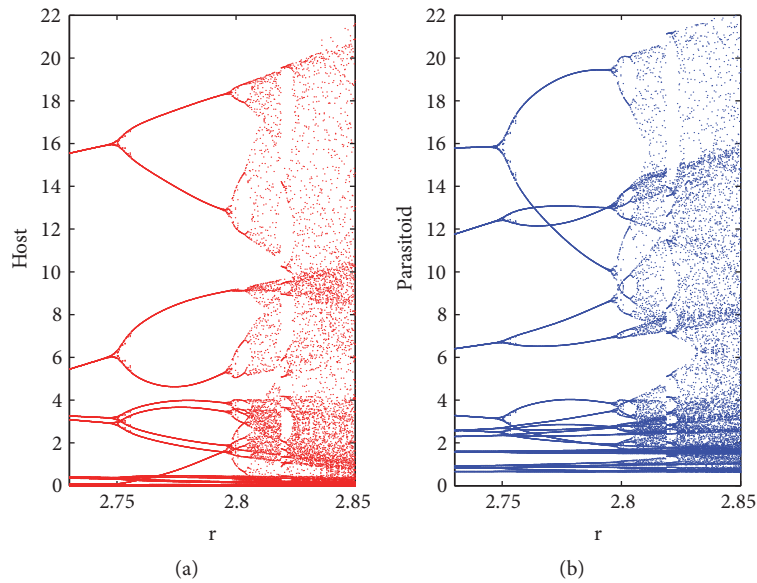


FIGURE 4: Bifurcation diagram of model (3) with  $r$ . Parameters are fixed as  $a = 0.45, \sigma = 0.4, q_1^{max} = 0.9, \theta_1 = 0.01, q_2^{max} = 0.1, \theta_2 = 0.5, \tau = 1.2, q = 2$ .

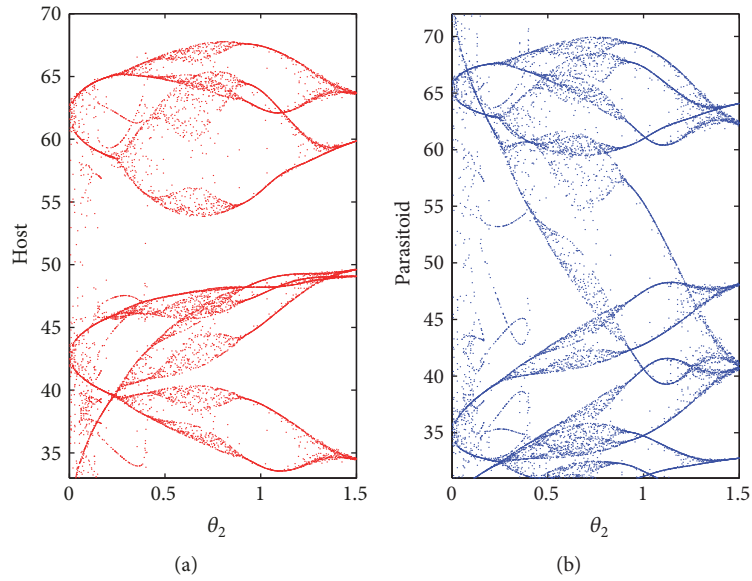


FIGURE 5: Bifurcation diagram of model (3) with  $\theta_2$ . Parameters are fixed as  $r = 0.8343$ ,  $a = 0.045$ ,  $\sigma = 0.5$ ,  $q_1^{max} = 0.5$ ,  $\theta_1 = 3$ ,  $q_2^{max} = 0.5$ ,  $\tau = 2$ ,  $q = 3$ .

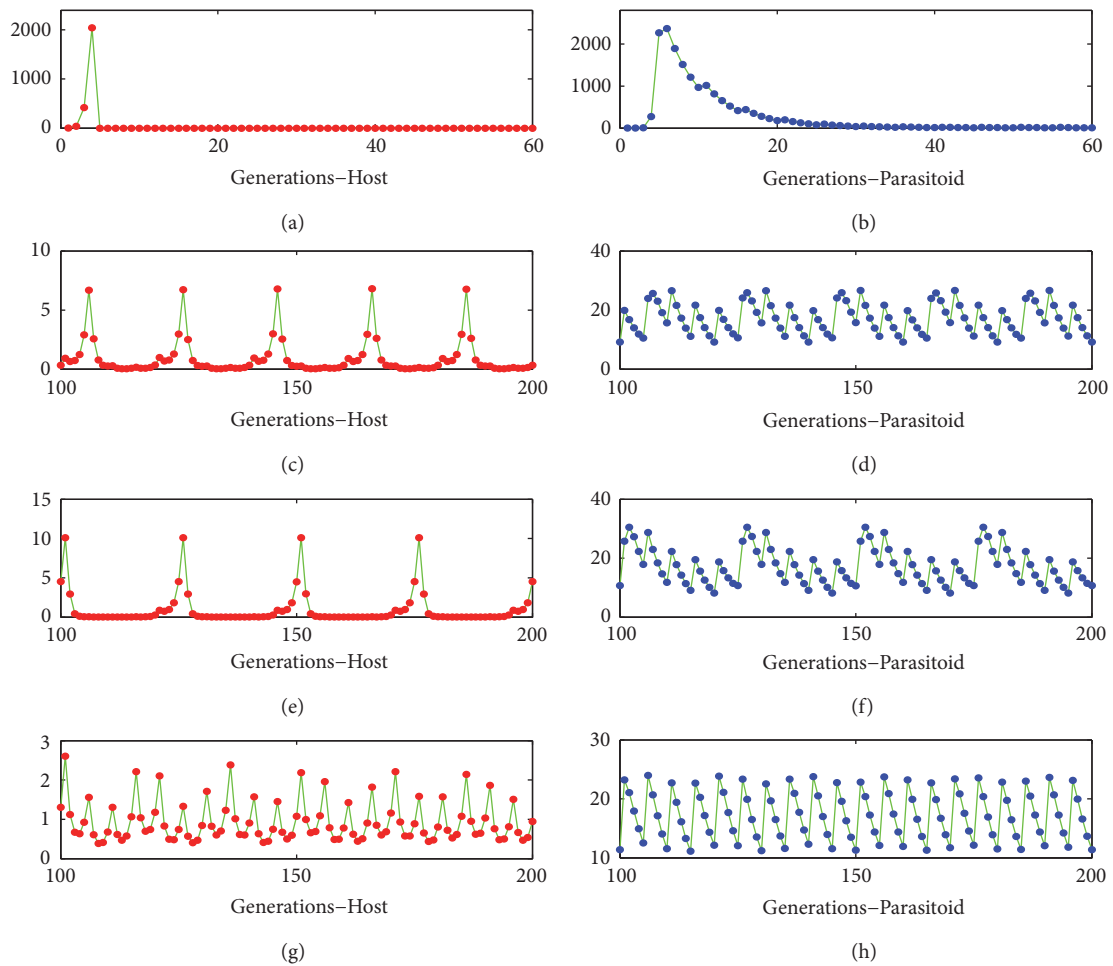


FIGURE 6: Four coexisting attractors of model (3). Parameters are  $r = 2.63$ ,  $a = 0.15$ ,  $q_1^{max} = 0.2$ ,  $\sigma = 0.8$ ,  $\theta_1 = 0.0001$ ,  $q_2^{max} = 0.3$ ,  $\theta_2 = 0.00005$ ,  $\tau = 10$ ,  $q = 5$ . The initial densities from top to bottom are  $(3.01, 0.99)$ ,  $(0.93, 20)$ ,  $(10.02, 25.81)$ ,  $(1, 25)$ , respectively.

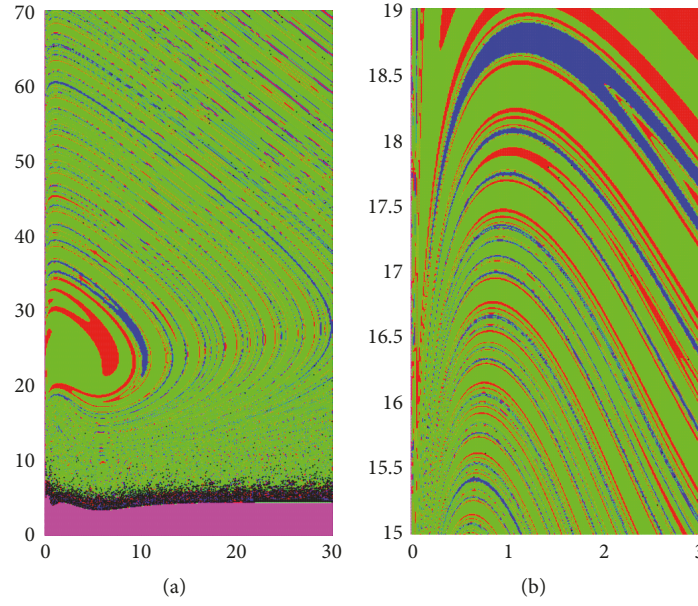


FIGURE 7: Basin of several attractions shown in Figure 6. The magenta, red, blue, and green points are attracted to the attractor shown in Figure 6 from top to bottom, respectively. The black points represent the other attractors not shown in Figure 6.

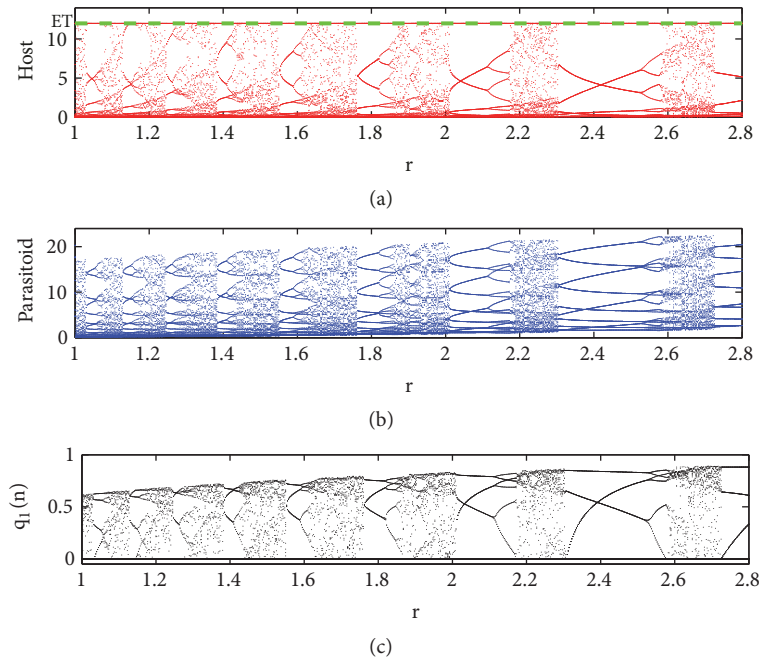


FIGURE 8: Bifurcation diagram of model (23) with  $r$ . Parameters are fixed as  $a = 0.25, \sigma = 0.6, q_2^{max} = 0.1, \theta_2 = 1, \tau = 2, ET = 12$ .

account; for convenience and simplification, then model (3) can be rewritten as

$$\begin{aligned}
 H_{n+1} &= \min \{H_n \exp [r - aP_n], ET\}, \\
 P_{n+1} &= H_n [1 - \exp (-aP_n)] + \sigma P_n, \\
 &\quad H_{n+1} \neq ET, n \in \mathcal{Z} \quad (23) \\
 P_{(n+1)^+} &= \left(1 + \frac{q_2^{max} P_n}{\theta_2 + P_n}\right) P_{n+1} + \tau, \quad H_{n+1} = ET
 \end{aligned}$$

with  $(H_{0^+}, P_{0^+}) = (H_0, P_0)$  and  $H_0 < ET$ . The term  $q_2^{max} P_n / (\theta_2 + P_n)$  represents the half-saturation function, and the parameters are the same as model (3).

**3.2. Numerical Bifurcation Analysis.** Compared with the fixed-time impulsive model (3), the state-dependent impulsive model (23) describes the threshold control policy and IPM strategy more complexly, and it is difficult to solve model (23) and especially in resource limitation model (23)

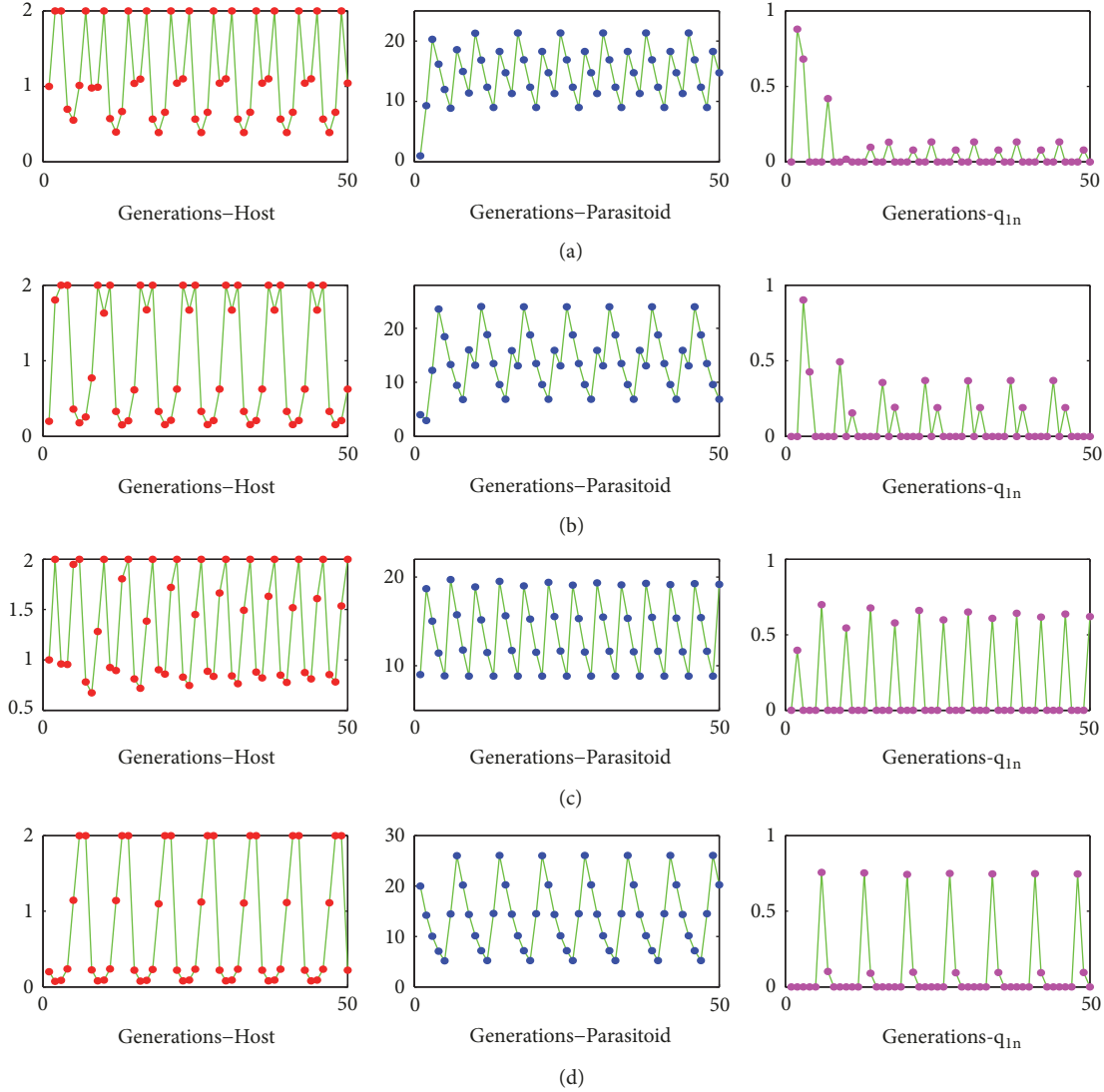


FIGURE 9: Four coexisting attractors of model (23). Parameters are  $r = 3$ ,  $a = 0.2$ ,  $\sigma = 0.7$ ,  $q_2^{max} = 0.5$ ,  $\theta_2 = 0.05$ ,  $\tau = 8$ ,  $ET = 2$ . The initial values from top to bottom are  $(1, 1)$ ,  $(0.2, 4)$ ,  $(1, 9)$ ,  $(0.2, 20)$ , respectively, and  $q_1(0) = 0$ .

becomes a complicated nonlinear dynamic system; it is difficult to investigate model (23) by theoretically, so we will investigate the dynamical behavior of model (23) by numerical simulations in the subsection and the analysis focus on the effects of some key parameters on dynamics of model (23) with limited resource.

Firstly, we choose the intrinsic growth rate  $r$  of hosts as a bifurcation parameter; the bifurcation diagrams of model (23) with the killing rate  $q_{1n}$  are derived. As shown in Figure 8, both populations  $H_n, P_n$  and the killing rate  $q_{1n}$  have quite interesting and complicated dynamics, including periodic doubling bifurcation, periodic window, chaotic solutions, and so on, when the intrinsic growth rate  $r$  varies from 1 to 2.8. The killing rate  $q_{1n}$  always oscillates between 0 and 1, which can pose a major challenge to be estimated and predicted.

Meanwhile, there are several types of solution including HF, HP periodic solutions, and HO solution; i.e., model (23) has several attractors with different initial densities. Figure 8

shows that model (23) has at least four different HP solutions or attractors. The maximum amplitudes of parasitoid population from top to bottom are 21.316, 23.996, 19.2084, 26.045, respectively; see Figures 9(a)–9(d) for details.

Furthermore, in order to illustrate the different initial densities that can cause the different dynamics, the basins of attractors are given in Figure 10. It shows that the dynamical behavior of model (23) and the host-killing rate  $q_{1n}$  are quite sensitive with varies of their initial value  $(H_0, P_0, q_{10})$ . Therefore, to successfully carry out a control pest plan, it is necessary to fully understand the initial state and analyze the changes in dynamics.

#### 4. Discussion and Conclusion

In order to investigate the effect of resource limitation on pest control, this paper develops two Nicholso-Bailey IPM

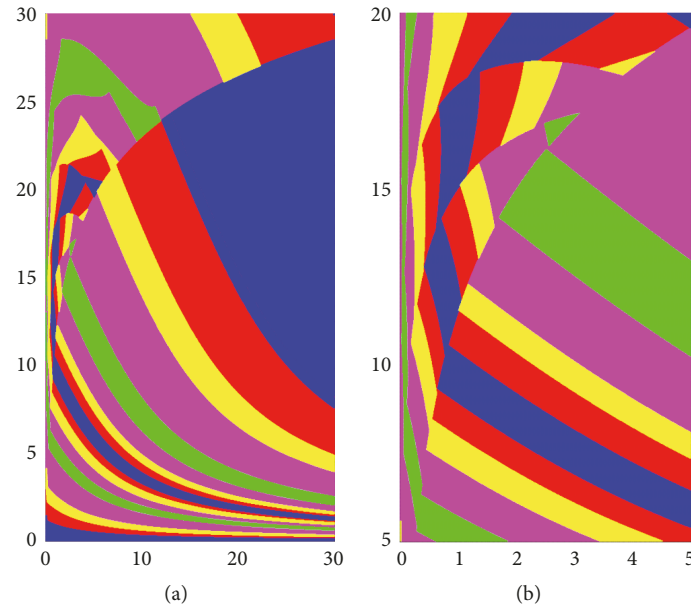


FIGURE 10: Basin of several attractions shown in Figure 9. The red, magenta, blue, and green points are attracted to the attractor shown in Figure 9 from top to bottom, respectively. The yellow points represent the other attractors not shown in Figure 9. All the parameters are identical to Figure 9. (b) is the magnification part of (a).

models with nonlinear impulsive control strategies. Theoretical, numerical, and biological analyses are given; those results show that it is critical to release parasitoid with an optimal number as the excessive releasing may cause intra-specific competition of parasitoid, which will seriously affect the pest control, especially for the limited resource. Meanwhile, the initial densities of both host and parasitoid populations can affect the pest outbreaks.

Model (3) describes the periodic control strategy, that is, a fixed-time impulsive control for a host-parasitoid model with resource limitation. According to the theoretical analysis, the existence and stability of host-free periodic solution of model (3) are derived; numerical threshold results show that we should take appropriate measures to prevent the releasing of parasitoid which will be beneficial to pest control, which is the optimal strategy to wrestle with enormous challenges of the limited resources. Meanwhile, numerical bifurcation results indicate that the nonlinear impulsive can make the dynamics of model (3) become more complex and interesting. There are several different bifurcation phenomena; we can find that the routes to chaos are very complicated; that is, there are several hidden factors that can adversely affect our control strategy. Those present a major challenge for controlling the pest populations in practice.

Model (23) describes the threshold control strategy in which measures could overcome the cost ineffectiveness or potentially damage to the environment in model (3). The threshold control strategy is to maintain the density of the hosts below the EIL rather than seeking to eradicate them, and the suitable tactic will be applied only as the density of hosts reaches the given ET. Numerical simulations clarify that the initial densities of both populations can affect the outcome of classical biological control, and the final stable

states of host and parasitoid populations depend on their initial densities. Those results are further confirmed by basins of attraction of initial densities.

This work only focuses on the limited resource; there are several other factors that can influence the pest control in reality, including Allee effect, delayed responses, and residual effects on hosts of pesticides. If those factors are considered, it will be of great theoretical and practical significance to investigate the effective prevention and control strategy for agricultural pests. Addressing these issues needs more future work.

### Data Availability

No data were used to support this study. In our study, there are only some numerical simulations to support our main result, and some parameter values to support the result of this paper are included within the article.

### Conflicts of Interest

The authors declare that there are no conflicts of interest regarding the publication of this article.

### Acknowledgments

This work was supported by National Natural Science Foundation of China (No. 11601268, Wenjie Qin); Educational Commission of Hubei Province (No. Q20161212, Wenjie Qin); China Scholarship Council to visit York University (No. 201808420192, Wenjie Qin); National Natural Science Foundation of China (No. 11761031, Guangyao Tang).

## References

- [1] H. A. Simon and A. J. Lotka, "Elements of mathematical biology," *Econometrica*, vol. 27, no. 3, p. 493, 1959.
- [2] L. Edelstein-Keshet, "Mathematical models in biology," *SIAM*, vol. 46, 1988.
- [3] J. D. Murray, *Mathematical Biology*, Springer, Berlin, Germany, 1989.
- [4] R. M. May, *Stability and Complexity in Model Ecosystems*, Princeton University Press, 1974.
- [5] H. I. Freedman, *Deterministic Mathematical Models in Population Ecology*, Marcel Dekker, New York, NY, USA, 1980.
- [6] R. P. Agarwal, *Difference Equations and Inequalities: Theory, Methods and Applications, Monographs Textbooks in Pure and Applied Mathematics*, Marcel Dekker, 2000.
- [7] S. Y. Tang and L. S. Chen, "Chaos in functional response host-parasitoid ecosystem models," *Chaos, Solitons & Fractals*, vol. 13, no. 4, pp. 875–884, 2002.
- [8] S. Y. Tang, Y. N. Xiao, and R. A. Cheke, "Multiple attractors of host-parasitoid models with integrated pest management strategies: eradication, persistence and outbreak," *Theoretical Population Biology*, vol. 73, no. 2, pp. 181–197, 2008.
- [9] C. Xiang, Z. Xiang, S. Tang, and J. Wu, "Discrete switching host-parasitoid models with integrated pest control," *International Journal of Bifurcation and Chaos*, vol. 24, no. 9, Article ID 1450114, pp. 1–20, 2014.
- [10] G. Livadiotis, L. Assas, B. Dennis, S. Elaydi, and E. Kwessi, "A discrete-time host-parasitoid model with an Allee effect," *Journal of Biological Dynamics*, vol. 9, no. 1, pp. 34–51, 2015.
- [11] F. Kangalgil and S. Kartal, "Stability and bifurcation analysis in a host-parasitoid model with Hassell growth function," *Advances in Difference Equations*, Paper No. 240, 15 pages, 2018.
- [12] D. Wu and H. Zhao, "Global qualitative analysis of a discrete host-parasitoid model with refuge and strong allee effects," *Mathematical Methods in the Applied Sciences*, vol. 41, no. 5, pp. 2039–2062, 2018.
- [13] Q. Din and M. Hussain, "Controlling chaos and Neimark-Sacker bifurcation in a host-parasitoid model," *Asian Journal of Control*, 2019.
- [14] V. Stern, R. Smith, R. Van den Bosch, and K. Hagen, "The integrated control concept," *Hilgardia*, vol. 29, no. 2, pp. 81–101, 1959.
- [15] J. C. Van Lenteren and J. Woets, "Biological and integrated pest control in greenhouses," *Annual Review of Entomology*, vol. 33, no. 1, pp. 239–250, 1988.
- [16] R. Van den Bosch, *The Pesticide Conspiracy*, University of California Press, 1989.
- [17] J. C. Van Lenteren, "Integrated pest management in protected crops, In Integrated pest management," in *Integrated pest management: principles and systems development*, pp. 311–320, Chapman & Hall, London, UK, 1995.
- [18] B. Liu, Y. Zhang, and L. Chen, "The dynamical behaviors of a Lotka-Volterra predator-prey model concerning integrated pest management," *Nonlinear Analysis: Real World Applications*, vol. 6, no. 2, pp. 227–243, 2005.
- [19] B. Liu, L. S. Chen, and Y. J. Zhang, "The dynamics of a prey-dependent consumption model concerning impulsive control strategy," *Applied Mathematics and Computation*, vol. 169, no. 1, pp. 305–320, 2005.
- [20] S. Y. Tang and R. A. Cheke, "State-dependent impulsive models of integrated pest management (IPM) strategies and their dynamic consequences," *Journal of Mathematical Biology*, vol. 50, no. 3, pp. 257–292, 2005.
- [21] S. Tang, Y. Xiao, L. Chen, and R. A. Cheke, "Integrated pest management models and their dynamical behaviour," *Bulletin of Mathematical Biology*, vol. 67, no. 1, pp. 115–135, 2005.
- [22] V. I. Utkin, *Sliding Modes and Their Applications in Variable Structure Systems*, Mir, 1978.
- [23] V. I. Utkin, *Sliding Modes in Control Optimization*, Springer, Berlin, Germany, 1991.
- [24] D. A. Andow and K. Kiritani, "The economic injury level and the control threshold," *Japan Pesticide Information*, vol. 43, p. 3, 1983.
- [25] L. P. Pedigo, S. H. Hutchins, and L. G. Higley, "Economic injury levels in theory and practice," *Annual Review of Entomology*, vol. 31, no. 1, pp. 341–368, 1986.
- [26] L. G. Higley and W. K. Wintersteen, "A novel approach to environmental risk assessment of pesticides as a basis for incorporating environmental costs into economic injury levels," *American Entomologist*, vol. 38, no. 1, pp. 34–39, 1992.
- [27] J. C. Headley, "Defining the economic threshold," in *Pest Control Strategies for the Future*, 1972.
- [28] H. C. Chiang, *General Model of the Economic Threshold Level of Pest Populations*, Plant Protection Bulletin, 1979.
- [29] M. J. Reynolds-Hogland, J. S. Hogland, and M. S. Mitchell, "Evaluating intercepts from demographic models to understand resource limitation and resource thresholds," *Ecological Modelling*, vol. 211, no. 3–4, pp. 424–432, 2008.
- [30] M. J. Reynolds-Hogland, L. B. Pacifici, and M. S. Mitchell, "Linking resources with demography to understand resource limitation for bears," *Journal of Applied Ecology*, vol. 44, no. 6, pp. 1166–1175, 2007.
- [31] W. Qin, S. Tang, and R. A. Cheke, "The effects of resource limitation on a predator-prey model with control measures as nonlinear pulses," *Mathematical Problems in Engineering*, vol. 2014, Article ID 450935, 13 pages, 2014.
- [32] W. Qin, S. Tang, C. Xiang, and Y. Yang, "Effects of limited medical resource on a Filippov infectious disease model induced by selection pressure," *Applied Mathematics and Computation*, vol. 283, pp. 339–354, 2016.
- [33] A. J. Nicholson and V. A. Bailey, "The balance of animal populations.—Part I," *Proceedings of the Zoological Society of London*, vol. 105, no. 3, pp. 551–598, 1935.
- [34] A. V. Hill, "The possible effects of the aggregation of the molecules of haemoglobin on its dissociation curves," *The Journal of Physiology*, vol. 40, no. 4, pp. 404–407, 1910.

